Development 136, 295-305 (2009) doi:10.1242/dev.027193

The bHLH transcription factor Olig3 marks the dorsal neuroepithelium of the hindbrain and is essential for the development of brainstem nuclei

Robert Storm[1,*], Justyna Cholewa-Waclaw[1,*], Katja Reuter[1,*], Dominique Bröhl[1], Martin Sieber[1,†], Mathias Treier[2], Thomas Müller[1] and Carmen Birchmeier[1,‡]

The *Olig3* gene encodes a bHLH factor that is expressed in the ventricular zone of the dorsal alar plate of the hindbrain. We found that the Olig3$^+$ progenitor domain encompassed subdomains that co-expressed Math1, Ngn1, Mash1 and Ptf1a. Olig3$^+$ cells give rise to neuronal types in the dorsal alar plate that we denote as class A neurons. We used genetic lineage tracing to demonstrate that class A neurons contribute to the nucleus of the solitary tract and to precerebellar nuclei. The fate of class A neurons was not correctly determined in *Olig3* mutant mice. As a consequence, the nucleus of the solitary tract did not form, and precerebellar nuclei, such as the inferior olivary nucleus, were absent or small. At the expense of class A neurons, ectopic Lbx1$^+$ neurons appeared in the alar plate in *Olig3* mutant mice. By contrast, electroporation of an Olig3 expression vector in the chick hindbrain suppressed the emergence of Lbx1$^+$ neurons. Climbing fiber neurons of the inferior olivary nucleus express Foxd3 and require *Olig3* as well as *Ptf1a* for the determination of their fate. We observed that electroporation of Olig3 and Ptf1a expression vectors, but not either alone, induced Foxd3. We therefore propose that Olig3 can cooperate with Ptf1a to determine the fate of climbing fiber neurons of the inferior olivary nucleus.

KEY WORDS: Fate mapping, Neuronal fate, Transcription factor, Mouse

INTRODUCTION

Brainstem neurons process and relay sensory information, control vital functions such as breathing and heart rate, and contribute to motor coordination (Blessing, 1997). The complex circuitry in which these neurons participate is established during development and depends on their spatially and temporally ordered appearance. The anlage of the hindbrain is segmented transiently into rhombomeres, and rhombomere borders align with the borders of expression of specific Hox genes (Fienberg et al., 1987; Wilkinson et al., 1989; Fraser et al., 1990; Krumlauf et al., 1993). Along the dorsoventral axis of the rhombomeres, specific neuronal types appear. Extensive cell migration and complex morphogenesis make it difficult to follow the destiny of distinct neuronal types in the hindbrain (Cobos et al., 2001; Dauger et al., 2003; Bloch-Gallego et al., 2005). Recent progress in genetic fate-mapping techniques that rely on the use of site-specific recombinases has helped to overcome this impediment (Branda and Dymecki, 2004; Joyner and Zervas, 2006). Combined with targeted mutations, genetic fate mapping can help to define the molecular determinants that control the development of brainstem nuclei.

One important class of genes that regulates cellular diversity in the nervous system encodes basic helix-loop-helix (bHLH) transcription factors. Early work demonstrated that bHLH factors act as generic proneural factors that function within the Notch pathway to single out neuronal progenitors and promote their differentiation. Subsequent analysis revealed the important roles of bHLH factors in the determination of neuronal fates (for reviews, see Brunet and Ghysen, 1999; Bertrand et al., 2002; Ross et al., 2003). The Olig genes encode a subfamily of bHLH transcription factors. The function of two family members, *Olig1* and *Olig2*, in the development of motoneurons and oligodendrocytes has been extensively characterized (Mizuguchi et al., 2001; Novitch et al., 2001; Zhou et al., 2001; Lu et al., 2002; Takebayashi et al., 2002a; Zhou and Anderson, 2002; Arnett et al., 2004). The third member, *Olig3*, is expressed in defined cell populations in the developing neural tube, among them dorsal progenitors (Takebayashi et al., 2002b). Recent work has demonstrated that *Olig3* expression in the spinal cord is controlled by dorsal patterning signals, and that *Olig3* is required to determine neuronal fates in the spinal cord of mice and zebrafish (Filippi et al., 2005; Muller et al., 2005; Zechner et al., 2007).

The dorsal ventricular zone of the medulla and pons generates brainstem nuclei, including the spinal trigeminal nucleus and the nucleus of the solitary tract that relay somatosensory and viscerosensory information, respectively, and precerebellar nuclei that function in motor coordination (Altman and Bayer, 1980; Altman and Bayer, 1987). Neurons that generate these nuclei migrate extensively before they settle, and arise from dorsal progenitor domains characterized by the expression of bHLH factors such as Math1 (Atoh1 – Mouse Genome Informatics), Ngn1 (Neurog1), Mash1 (Ascl1) and Ptf1a (Pattyn et al., 2000; Qian et al., 2001; Landsberg et al., 2005; Wang et al., 2005; Sieber et al., 2007; Yamada et al., 2007). For instance, neurons of the lateral reticular, external cuneate, pontine and reticulotegmental nuclei arise from Math1$^+$ progenitors at the dorsal lip, and Math1 is required to determine their fate (Bermingham et al., 2001; Machold and Fishell, 2005; Wang et al., 2005). These neurons express the homeodomain factors Barhl1/2 and Lhx2/9, and depend on these factors for differentiation (Saito et al., 1998; Bermingham et al., 2001; Li et al., 2004). Mash1$^+$ progenitors locate further ventrally and appear to give rise to neurons of the nucleus of

[1]Max-Delbrück-Centrum for Molecular Medicine, Robert-Rössle-Strasse 10, 13125 Berlin, Germany. [2]EMBL, Meyerhofstrasse 1, 69117 Heidelberg, Germany.

*These authors contributed equally to this work
†Present address: Bayer Schering Pharma AG, 13353 Berlin, Germany
‡Author for correspondence (cbirch@mdc-berlin.de)

Accepted 6 November 2008

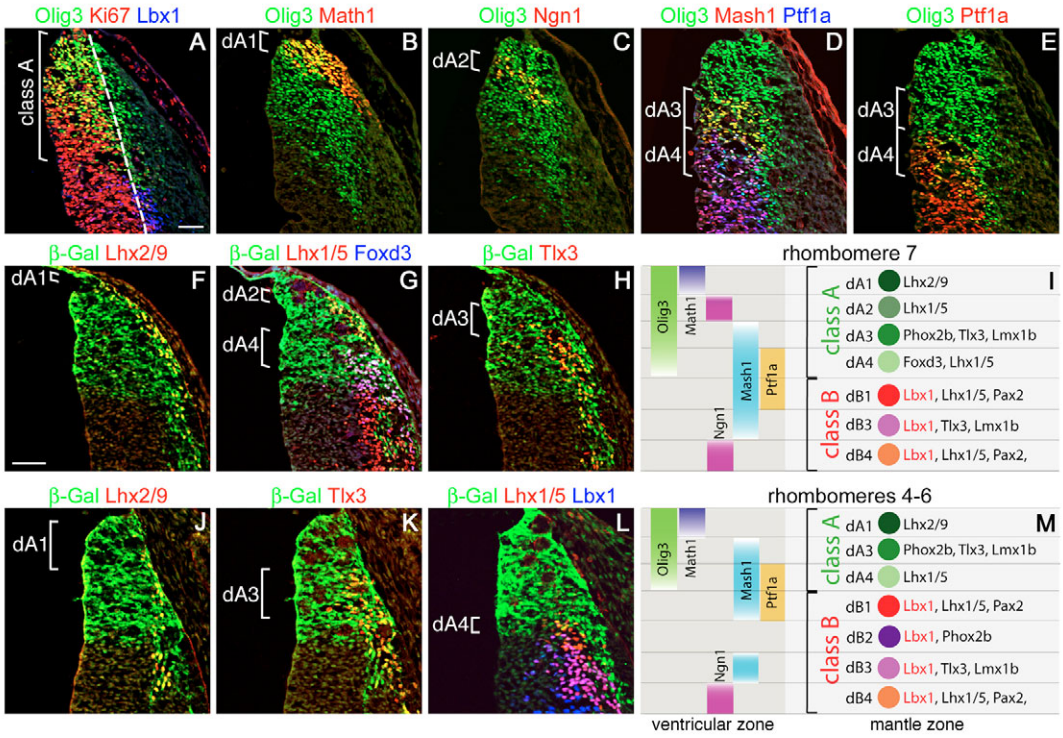

Fig. 1. Characterization of neuronal subtypes that arise from Olig3$^+$ cells in the mouse dorsal hindbrain. (**A-E**) Immunohistological analysis of Olig3$^+$ cells on consecutive sections of the dorsal alar plate of rhombomere 7 at E11.5. Olig3$^+$ cells were observed in a broad domain of the ventricular zone. See Fig. S1A in the supplementary material for an explanation of the sector displayed. Immunohistological analysis of (A) Olig3, Ki67 and Lbx1, (B) Olig3 and Math1, (C) Olig3 and Ngn1, (D) Olig3, Mash1 and Ptf1a, (E) Olig3 and Ptf1a. Note that D and E show the same section; in E, the Mash1 signal was removed, and the Ptf1a signal is shown in red. (**F-H**,**J-L**) Analysis of neuronal types generated by Olig3$^+$ cells using genetic lineage tracing in rhombomere 7 (F-H) and rhombomeres 4-6 (J-L). Recombination was induced in *Olig3$^{CreERT2/+}$*; *Rosa26R* mice at E9.5 by tamoxifen; cells that expressed the active *lacZ* gene were identified using anti-β-Gal antibodies. Neuronal types were defined using antibodies against Lhx2/9 (F,J), Lhx1/5 and Foxd3 (G), Tlx3 (H,K), and Lhx1/5 and Lbx1 (L). Note that J and K show the same section, which was stained for β-Gal, Lhx2/9 and Tlx3; J and K display β-Gal/Lhx2/9 and β-Gal/Tlx3 signals, respectively. (**I**,**M**) The distinct dorsal ventricular zones and neuronal subtypes of rhombomeres 7 (I) and 4-6 (M) (Sieber et al., 2007). Scale bars: 50 μm.

the solitary tract, as these are generated in reduced numbers in *Mash1* mutant mice (Dauger et al., 2003; Pattyn et al., 2006). Neurons of the nucleus of the solitary tract express the homeodomain factors Phox2b and Tlx3, and depend on these for differentiation (Qian et al., 2001; Dauger et al., 2003). Neurons of the inferior olivary nucleus arise from a Ptf1a$^+$ ventricular zone located further ventrally, and Ptf1a is required to determine their fate (Yamada et al., 2007).

We have defined Olig3 expression in the mouse dorsal hindbrain, and show here that the Olig3$^+$ domain of the ventricular zone overlaps with the Math1, Ngn1 and dorsal aspects of the Mash1 and Ptf1a expression domains. Lineage tracing demonstrated that Olig3-derived cells contribute to the nucleus of the solitary tract and to precerebellar nuclei, such as the inferior olivary nucleus. Analysis of *Olig3* mutant mice revealed that the precerebellar nuclei and the nucleus of the solitary tract were either absent or small. Finally, we observed that Olig3 and Ptf1a cooperate in neuronal fate determination, and that co-electroporation of Olig3 and Ptf1a expression vectors induced Foxd3, a molecular characteristic of climbing fiber neurons of the inferior olivary nucleus.

MATERIALS AND METHODS

Mouse strains

The *Olig3CreERT2* allele was generated by homologous recombination in embryonic stem (ES) cells. *CreERT2* (Feil et al., 1997) replaces the *Olig3* coding sequence and was fused in frame with the ATG codon of *Olig3*. In addition, the neomycin resistance gene (*neo*) flanked by *FRT* sites was inserted. Mutant ES cells were used to generate a mouse strain, and *neo* was removed by crossing with FLPe deleter mice (Farley et al., 2000). To induce Cre-mediated recombination, tamoxifen (Sigma-Aldrich; 20 mg/ml in sunflower oil) was administered to pregnant females at 100 mg/kg (Joyner and Zervas, 2006). The generation of *Rosa26R* and *Olig3^{null}* mice has been described (Soriano, 1999; Muller et al., 2005).

Anatomy, immunohistology, in situ hybridization, microscopy and in ovo electroporation

Rhombomeric units were identified using morphological landmarks such as hindbrain nuclei and exit points of cranial nerves (Marin and Puelles, 1995; Cambronero and Puelles, 2000). Antibodies used were: guinea pig and rabbit anti-Olig3 (Muller et al., 2005), rabbit anti-Foxd3 (Martyn Goulding, Salk Institute, La Jolla, CA), guinea pig anti-Foxd3 (Muller et al., 2005), rabbit anti-Brn3a (Eric Turner, UCSD, La Jolla, CA), guinea pig anti-Tlx3 and anti-Lbx1 (Muller et al., 2002), chick anti-β-galactosidase (Abcam, Poole, UK), mouse anti-Mash1 (BD Biosciences Pharmingen), rabbit anti-Phox2b (Christo Goridis and Jean-Francois Brunet, Ecole Normale Superieure, Paris, France), mouse anti-NF68 (Sigma, Munich, Germany), rabbit anti-Pax2 (Zymed, San Francisco, CA), guinea pig anti-Ptf1a and rabbit anti-Ngn1 (Jane Johnson, Southwestern Medical Center, Dallas, TX), mouse anti-Lhx1/5 and anti-Pax7 (DSHB, University of Iowa, IA), rabbit anti-Lhx2/9 and anti-Math1 (Tom Jessell, Columbia University, New York, NY), rabbit anti-Cre (Novagen). Cy2-, Cy3- and Cy5-conjugated secondary antibodies were obtained from Dianova (Hamburg, Germany). Fluorescence was

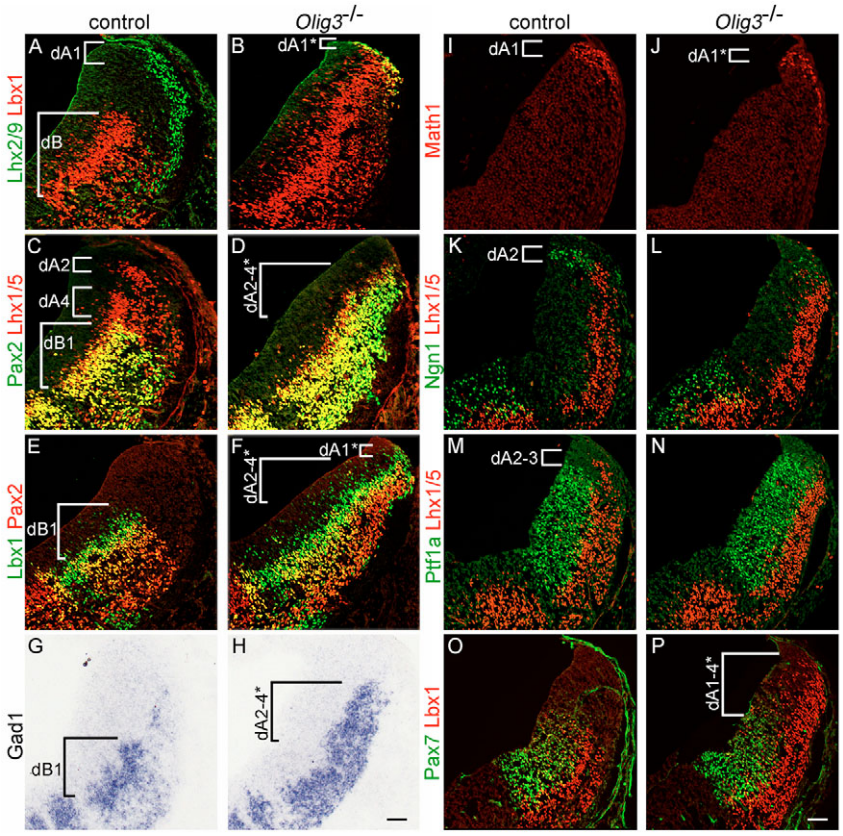

Fig. 2. Olig3 is required to determine the fate of class A neurons in rhombomere 7. Immunohistological (A-F,I-P) and in situ hybridization (G,H) analyses of the alar plate of rhombomere 7 of control and *Olig3* mutant mice at E11.5. (**A**,**B**) In control animals (A), Lbx1$^+$ neurons were restricted to the ventral alar plate, and Lhx2/9$^+$ neurons (dA1) arose at the dorsal lip. In *Olig3* mutant mice (B), Lbx1$^+$ neurons arose throughout the entire alar plate, and Lhx2/9$^+$ neurons (dA1*) co-expressed Lbx1. (**C-F**) Pax2 and Lhx1/5 (C,D) and Lbx1 and Pax2 (E,F) expression. (**G**,**H**) Analysis using a *Gad1*-specific probe. (**I-P**) Analyses using antibodies against Math1 (I,J), Ngn1 and Lhx1/5 (K,L), Ptf1a and Lhx1/5 (M,N) and Pax7 and Lbx1 (O,P). Note the expanded expression of Ptf1a in the *Olig3* mutant mice. Distinct neuronal subtypes are indicated. Scale bars: 50 μm.

visualized by laser-scanning microscopy (LSM 5 PASCAL, Carl-Zeiss, Germany), using PASCAL software. For the display of overviews, pictures were merged using Adobe Photoshop.

The number of Pax2$^+$ neurons on sections was determined using a program developed by Bartlomiej Waclaw (Institut für Theoretische Physik, Universität Leipzig, Leipzig, Germany). The program, which counts bright, oval-shaped objects in two-dimensional pictures, relies on a method similar to the one described by Byun et al. (Byun et al., 2006), and is available at http://www.physik.uni-leipzig.de/~waclaw/count/index.html. Three sections from three different animals each were analyzed.

In situ hybridization and chick in ovo electroporation were performed as described (Brohmann et al., 2000; Dubreuil et al., 2002). Neuron numbers on the electroporated and control sides were counted on three caudal brainstem sections from three electroporated embryos. Morphometric analysis was performed on serial hindbrain sections stained by in situ hybridization with a *Barhl1*-specific probe. *Barhl1*-positive areas were measured on every second section to determine the volume of external cuneate and lateral reticular nuclei using ImageJ (W. S. Rasband, NIH, Bethesda, MD).

RESULTS

Defining neuronal subtypes that arise from Olig3$^+$ cells in rhombomeres 4-7

The expression of the murine bHLH gene *Olig3* is first detected around embryonic day 9.25 (E9.25) in the dorsal hindbrain and spinal cord (Takebayashi et al., 2002b; Ding et al., 2005; Muller et al., 2005). We used immunohistochemistry to characterize Olig3$^+$ cells on transverse sections of the hindbrain. At E11.5, we observed Olig3$^+$ cells in a broad domain that extended from the roof plate ventrally (Fig. 1A-E, showing the alar plate). The majority of these Olig3$^+$ cells were located in the ventricular zone, but Olig3 was also detected in a stripe of cells located in the mantle zone (Fig. 1A; see Fig. S1A-D in the supplementary material). This indicates that Olig3 is expressed by progenitors and postmitotic neurons. Further analysis showed that Olig3$^+$ cells of the ventricular zone were heterogeneous. In rhombomere 7, Olig3$^+$ cells close to the roof plate co-expressed Math1 (Fig. 1B). Ventrally abutting Olig3$^+$ cells co-expressed Ngn1 (Fig. 1C). Two further ventrally located domains were defined, one that contained cells co-expressing Olig3 and Mash1, and a second containing cells that expressed Olig3, Mash1 and Ptf1a (Fig. 1D,E). Thus, we defined four distinct ventricular subdomains containing Olig3$^+$ cells (see Fig. 1I for a summary). The majority of the cells in the dorsal subdomain were Olig3$^+$, whereas in ventrally located subdomains only a fraction expressed Olig3 (Fig. 1A-E). In dorsal ventricular subdomains, Ki67, a marker for proliferation, was co-expressed with Olig3; in ventrally located subdomains, Ki67$^+$ cells rarely co-expressed Olig3 (Fig. 1A). Thus, cells in different subdomains of the ventricular zone appear to express Olig3 in distinct phases of the cell cycle. At later developmental stages, for instance E12.5, the dorsal Olig3$^+$ domain was markedly smaller than at earlier stages (data not shown). In rhombomeres 4-6, subdomains containing cells that express Olig3/Math1, Olig3/Mash1 and Olig3/Mash1/Ptf1a were observed (not shown). In accordance with previous reports (Landsberg et al., 2005), a dorsal Ngn1$^+$ ventricular domain in rhombomeres 4-6 was not found (data not shown; see Fig. 1M for a summary).

We used the *Olig3^{CreERT2}* allele (see below for details of the allele) and a *lacZ* reporter (*Rosa26R*) for genetic lineage tracing, and a panel of antibodies to characterize neurons that derive from Olig3$^+$ cells. Derivatives of cells in which recombination has occurred inherit the active *lacZ* allele and express β-galactosidase (β-Gal). The most dorsal β-Gal$^+$ neuronal population detected, dA1, co-expressed Lhx2/9 (Fig. 1F). Ventral to these cells, β-Gal$^+$ dA2 and dA4 neurons were observed; dA2 neurons co-expressed Lhx1/5, whereas dA4 neurons co-expressed Lhx1/5 and Foxd3 (Fig. 1G). In addition, we detected β-Gal$^+$ dA3 neurons that co-expressed Tlx3 [Fig. 1H; note

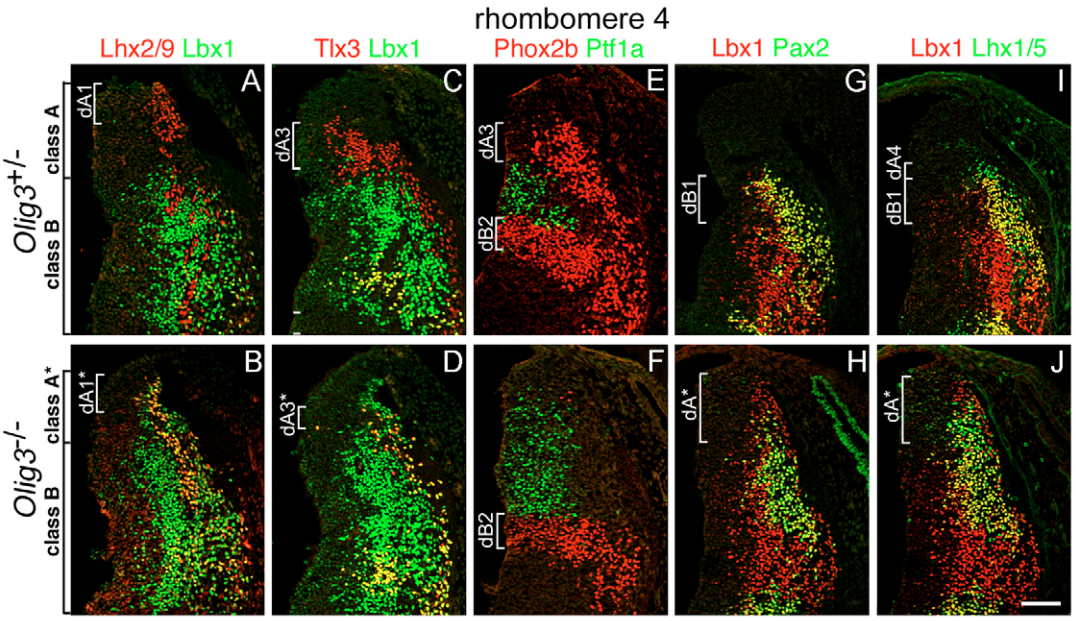

Fig. 3. Olig3 is required to determine the fate of class A neurons in rhombomere 4. Immunohistological analyses (antibodies as labeled) of the alar plate of rhombomere 4 of control (*Olig3*$^{+/-}$) and *Olig3* homozygous mutant mice at E11.5. (**A**,**B**) In control animals, Lbx1^{+} neurons were restricted to the ventral alar plate. In *Olig3* mutant mice, ectopic Lbx1^{+} neurons were present. (**C**,**D**) In *Olig3* mutant mice, Tlx3^{+} (dA3*) neurons were generated in reduced numbers and co-expressed Lbx1. (**E**,**F**) Phox2b^{+} dA3 neurons were not present in *Olig3* mutant mice, and the expression domain of Ptf1a was expanded. (**G-J**) In the dorsal alar plate of *Olig3* mutant mice, Lhx1/5^{+}/Lbx1^{+}, Lhx1/5^{+}/Lbx1^{-} and Lbx1^{+}/Pax2^{+} neurons arose in an apparently intermingled manner. Note that G,I and H,J show identical sections, which were stained with antibodies against Lbx1, Pax2 and Lhx1/5; G,H and I,J display Lbx1/Pax2 and Lbx1/Lhx1/5 signals, respectively. Scale bar: 50 μm.

that Tlx3^{+} neurons also express Phox2b and Lmx1b, see Fig. 7A and Sieber et al. (Sieber et al., 2007)]. Foxd3^{+} dA4 neurons were located lateral to the ventricular zone that contained Olig3^{+}, Mash1^{+} and Ptf1a^{+} cells (see Fig. S1E-G in the supplementary material). Others previously characterized Math1^{+}, Ngn1^{+}, Mash1^{+} and Ptf1a^{+} ventricular subdomains and the neuronal types they generate (Bermingham et al., 2001; Qian et al., 2001; Landsberg et al., 2005; Machold and Fishell, 2005; Wang et al., 2005; Pattyn et al., 2006; Yamada et al., 2007). Thus, Olig3^{+} cells generate four dorsal neuronal subtypes in rhombomere 7, and these appear to arise from ventricular subdomains that contain cells expressing Olig3/Math1, Olig3/Ngn1, Olig3/Mash1 and Olig3/Mash1/Ptf1a (summarized in Fig. 1I).

We defined neurons derived from Olig3^{+} cells in more-rostral rhombomeres at E11.5. The most dorsal β-Gal^{+} neuronal population co-expressed Lhx2/9 (dA1, Fig. 1J) and arose in all segments of the hindbrain; this population has been extensively characterized previously (Bermingham et al., 2001; Machold and Fishell, 2005; Wang et al., 2005). Ventral to these cells, β-Gal^{+}/Tlx3^{+} (dA3) neurons were observed, which co-express Phox2b and Lmx1b and were present in rhombomeres 4-7 but not in more-rostral rhombomeres (Fig. 1H,K, Fig. 3C,E and data not shown) (Pattyn et al., 2000; Qian et al., 2001; Dauger et al., 2003; Sieber et al., 2007). We identified an additional, small β-Gal^{+} cell population located further ventrally that expressed Lhx1/5^{+} (dA4); dA4 neurons of rhombomere 7, but not of rhombomeres 4-6, co-expressed Foxd3 (Fig. 1G,L and data not shown).

Olig3 antagonizes the development of class B neurons

During normal development of rhombomere 7, class A neurons arise in the dorsal alar plate and Lbx1^{+} class B neurons in the ventral alar plate (Fig. 2A,C,E) (Sieber et al., 2007). We observed a pronounced dorsal expansion of Lbx1^{+} neurons in *Olig3* mutant mice in rhombomere 7 (Fig. 2B). Most ectopic Lbx1^{+} neurons co-expressed Pax2 and Lhx1/5, and we denote these as dA2-4* (Fig. 2B,D,F). In normal development, Lbx1^{+}/Pax2^{+} neurons of the dorsal spinal cord and hindbrain express glutamic acid decarboxylase 1 (Gad1), an enzyme essential for GABA synthesis (Cheng et al., 2005) and these neurons arise exclusively in the ventral alar plate (Fig. 2G). In *Olig3* mutants, Gad1^{+} neurons arose ectopically in the dorsal alar plate (Fig. 2H). We conclude that dA2-dA4 neurons are not correctly specified in rhombomere 7 of *Olig3* mutant mice. At their expense, Gad1^{+}/Lbx1^{+}/Pax2^{+}/Lhx1/5^{+} neurons arose that displayed molecular characteristics of inhibitory neurons. We identified an additional aberrant neuronal subtype close to the roof plate in *Olig3* mutants; these neurons co-expressed Lbx1 and Lhx2/9, and we denote them as dA1* (Fig. 2B).

We analyzed genes expressed in the dorsal ventricular zone of rhombomere 7 in *Olig3* mutant mice. Compared with control animals, Math1 and Ngn1 expression was reduced in *Olig3* mutants (Fig. 2I-L). By contrast, Ptf1a expression was expanded dorsally (Fig. 2M,N). Pax7 and Mash1 were similarly expressed in control and *Olig3* mutant mice (Fig. 2O,P and data not shown). We conclude that *Olig3* is essential to maintain the correct expression of Math1, Ngn1 and Ptf1a in the dorsal ventricular zone of rhombomere 7.

In rhombomeres 4-6 of *Olig3* mutant mice, we also observed a pronounced dorsal expansion of Lbx1^{+} neurons (Fig. 3A-D). Close to the roof plate, we identified neurons that co-expressed Lhx2/9 and Lbx1 (dA1*, Fig. 3B). Tlx3^{+}/Phox2b^{+} dA3 neurons were not present, and instead we observed Tlx3^{+}/Lbx1^{+} (dA3*) neurons, which appeared to intermingle with Lbx1^{+}/Pax2^{+} and Lhx1/5^{+}/Lbx1^{-} neurons (Fig. 3C-J). These changes were accompanied by a dorsal expansion of Ptf1a (Fig. 3E,F). It should be noted that in the alar plate of rhombomeres 4-6, our panel of

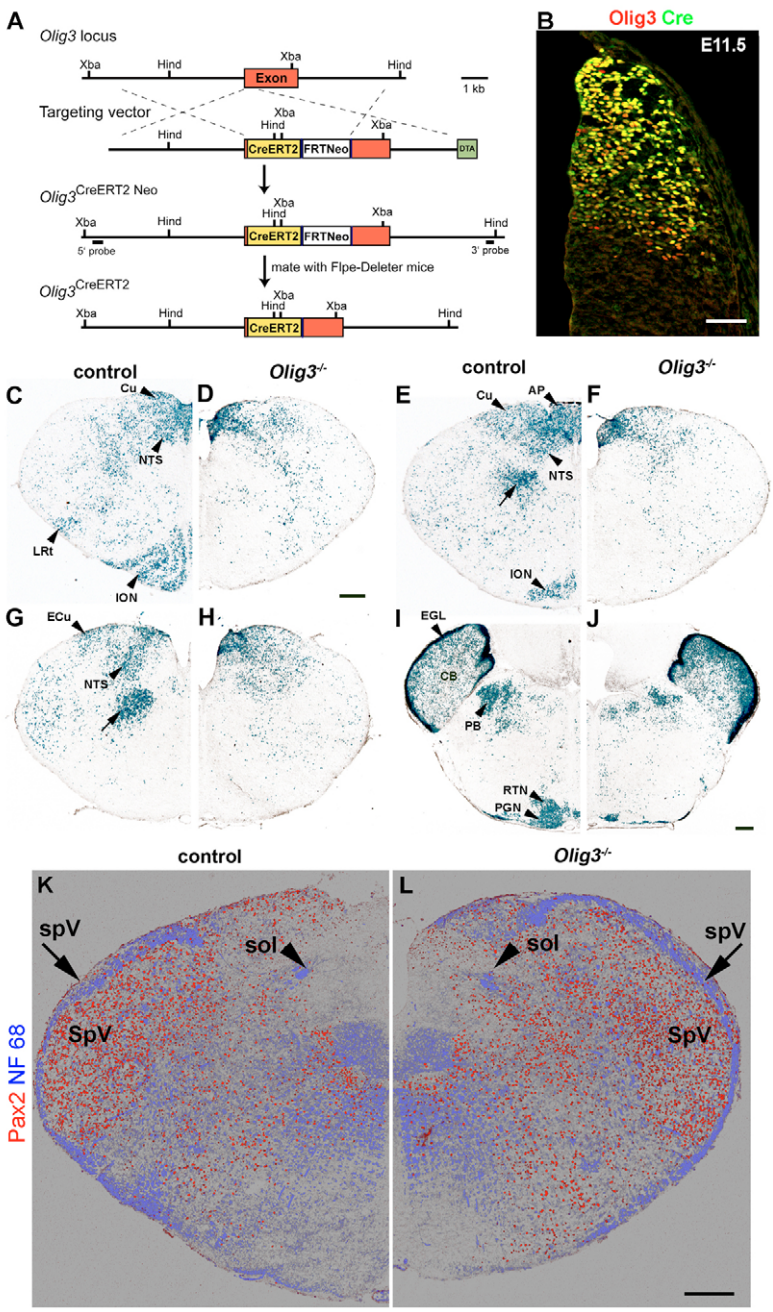

Fig. 4. Genetic lineage tracing in heterozygous and homozygous *Olig3* mutant mice. (**A**) Strategy used to generate the *Olig3*^{CreERT2} allele. Schematic representation of the wild-type *Olig3* locus, the targeting vector, and the mutant *Olig3* alleles before (*Olig3*^{CreERT2neo}) and after (*Olig3*^{CreERT2}) removal of the *neomycin* (*neo*) cassette. The coding exon of *Olig3* (red) was interrupted by the insertion of a *CreERT2-FRT-neo-FRT* cassette. Indicated are *CreERT2* (yellow) and the *neo* resistance cassette surrounded by *FRT* sequences (*FRT-neo-FRT*); in addition, a *diphtheria toxin A* (*DTA*, light green) cassette was included for negative selection. (**B**) Immunohistological analysis of rhombomere 7 in *Olig3*$^{CreERT2/+}$ mice at E11.5 using antibodies against Cre and Olig3. (**C-J**) Analysis of the medulla oblongata and pons of control (*Olig3*$^{CreERT2/+}$; *Rosa26R*) and *Olig3* mutant (*Olig3*$^{CreERT2/–}$; *Rosa26R*) mice at E18.5. Recombination was induced at E10.5 by tamoxifen, and expression of the active *lacZ* gene was identified by X-Gal staining (blue). (**K**,**L**) Immunohistological analysis using antibodies against Pax2 and NF68 (Nefl). To improve the visibility of neurons, a false color was assigned to the black background of the original photograph. Arrowheads and arrows indicate the solitary (sol) and spinal trigeminal (spV) tracts, respectively. Cu, cuneate nucleus; ECu, external cuneate nucleus; ION, inferior olivary nucleus; NTS, nucleus of the solitary tract; LRt, lateral reticular nucleus; PB, parabrachial nucleus; PGN, pontine gray nucleus; RTN, reticulotegmental nucleus; CB, cerebellum; EGL, external granular layer. Scale bars: 50 μm in B; 200 μm in D,J,L.

markers defined identical neuronal subtypes in control and mutant mice, and we display exemplary data on rhombomere 4. Thus, loss of *Olig3* results in expanded expression of Lbx1 and Ptf1a in rhombomeres 4-7. No apparent ectopic Lbx1 expression was observed in rhombomeres 1-3, as assessed by immunohistology and whole-mount in situ hybridization (data not shown). We therefore restricted subsequent analyses to rhombomeres 4-7 and their derivatives.

Derivatives of Olig3^{+} cells

We used genetic lineage tracing and the *Olig3*^{CreERT2} allele to follow the fate of Olig3^{+} cells (see Fig. 4A for targeting strategy and the structure of *Olig3*^{CreERT2}). Analysis of the alar plate of *Olig3*$^{CreERT2/+}$ mice demonstrated that Cre and Olig3 were co-expressed in many cells (Fig. 4B). A few cells did not co-express Cre and Olig3, which might reflect differences in the stability of the two proteins. For fate-mapping experiments in *Olig3* heterozygous and homozygous mutant mice (*Olig3*$^{CreERT2/+}$; *Rosa26R* and *Olig3*$^{CreERT2/–}$; *Rosa26R*), we induced recombination at E10.5 and identified recombined cells and their derivatives by β-Gal expression (X-Gal staining on sections). In the caudal medulla oblongata of heterozygous mutant mice at E18.5, β-Gal^{+} cells were present in the cuneate nucleus, the nucleus of the solitary tract, the lateral reticular nucleus, and the inferior olivary nucleus (Fig. 4C). Further rostrally, β-Gal^{+} cells were observed in the area postrema (Fig. 4E), the external cuneate nucleus (Fig. 4G), as well as in the reticulotegmental, pontine gray and parabrachial nuclei (Fig. 4I). We also observed β-Gal^{+} cells in the reticular formation (Fig. 4E,G, arrows) and in the cerebellum (Fig. 4I). In homozygous *Olig3* mutants, β-Gal^{+} cells were either absent or present in reduced numbers at the position of the lateral

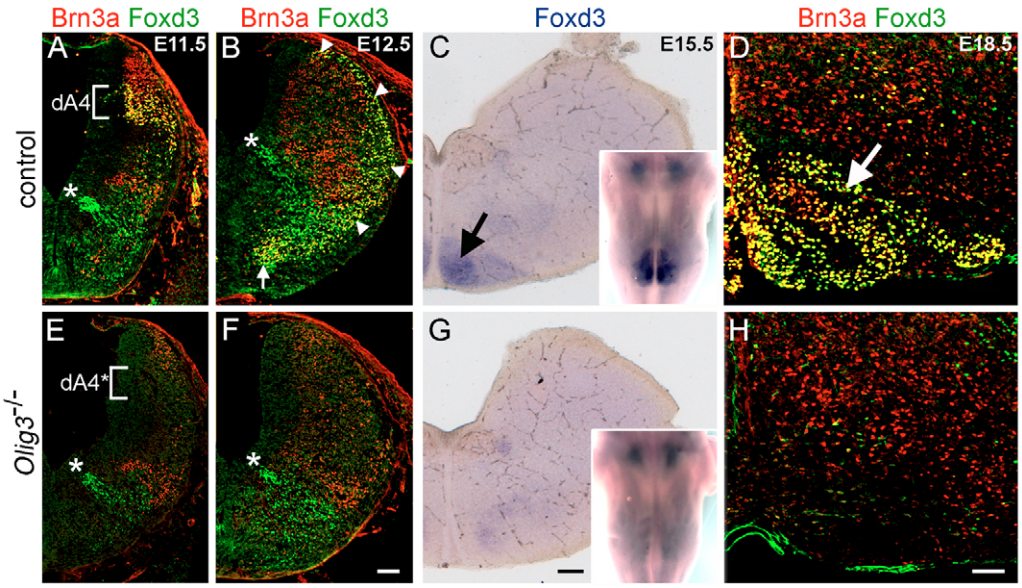

Fig. 5. dA4 neurons and their derivative, the inferior olivary nucleus, are absent in *Olig3* mutant mice. (**A**,**B**,**D**,**E**,**F**,**H**) Immunohistological analysis of control (A,B,D) and *Olig3* mutant (E,F,H) mice using antibodies against Brn3a and Foxd3. In control mice at E11.5 (A), Brn3a$^+$/Foxd3$^+$ dA4 neurons emerged in the dorsal alar plate. Foxd3/Brn3a co-expression marks specifically dA4; other neuronal types expressed either Foxd3 (a ventral population, asterisk) or Brn3a (dorsal neuronal subtypes). At E12.5 (B), a stream of Foxd3$^+$/Brn3a$^+$ dA4 neurons (arrowheads) extended ventrally and appeared to assemble close the ventral midline (arrow). In *Olig3* mutant mice at E11.5 (E) and at E12.5 (F), Foxd3$^+$/Brn3a$^+$ dA4 neurons were absent. At E18.5. Foxd3$^+$/Brn3a$^+$ neurons were located in the inferior olivary nucleus of control mice (arrow, D), but were absent in *Olig3* mutants (H). (**C**,**G**) In situ hybridization analysis of control (C) and *Olig3* mutant (G) mice at E15.5 using a *Foxd3*-specific probe (arrow in C). The insets show the whole-mount in situ hybridization of the corresponding hindbrains prior to sectioning. Scale bars: 50 μm in F,G; 100 μm in H.

reticular, inferior olivary, external cuneate, reticulotegmental, pontine gray and parabrachial nuclei (Fig. 4C-J). In the dorsomedial domain, where the nucleus of the solitary tract, the area postrema and the cuneate nucleus are located in normal development, the medullary morphology was altered in *Olig3* mutant mice, and β-Gal$^+$ cells were distributed in an aberrant manner (Fig. 4C-J).

Supernumerary inhibitory Lbx1$^+$/Pax2$^+$ neurons were observed at E11.5 in rhombomere 7, and we tested whether these were retained. We found that the number of Pax2$^+$ neurons on sections of the caudal medulla oblongata was significantly increased at E18.5 (Fig. 4K,L): we counted 4027±201 and 5611±229 Pax2$^+$ neurons/section in heterozygous versus homozygous mutant mice, respectively. We also observed an increased number of Gad1$^+$ neurons in homozygous as compared with heterozygous *Olig3* mutant mice (see Fig. S2 in the supplementary material). Thus, supernumerary Pax2$^+$ inhibitory neurons persisted in the caudal medulla oblongata, and were still detectable at E18.5 in *Olig3* mutant mice.

We followed various class A neuronal subtypes in *Olig3* mutant mice. In control mice, dA4 neurons of rhombomere 7 co-expressed Brn3a (Pou4f1 – Mouse Genome Informatics) and Foxd3 at E11.5 (Fig. 5A). The Brn3a$^+$/Foxd3$^+$ dA4 neurons migrated tangentially, forming a stream that extended at E12.5 into the ventral hindbrain, and they settled close to the midline (Fig. 5B). At E15.5 and E18.5, Foxd3$^+$ neurons were observed close to the ventral midline, and by E18.5 the Brn3a$^+$/Foxd3$^+$ neurons assembled in the characteristic structure of the inferior olivary nucleus (Fig. 5C,D). In *Olig3* mutant mice, Brn3a$^+$/Foxd3$^+$ neurons were absent at E11.5, and at E12.5 the ventrally migrating stream of Foxd3$^+$/Brn3a$^+$ neurons was lacking (Fig. 5E,F). At E15.5, Foxd3$^+$ neurons at the ventral midline were absent, and we did not detect Foxd3$^+$/Brn3a$^+$ neurons at the position of the inferior olivary nucleus at E18.5 (Fig. 5G,H). Histological analysis confirmed the absence of the characteristic structure of the inferior olivary nucleus (data not shown; see also Fig. 4C,D and Fig. 5D,H). We conclude that the fate of dA4 neurons is not correctly determined in *Olig3* mutant mice, resulting in the absence of climbing fiber neurons of the inferior olivary nucleus.

Foxd3$^+$ climbing fiber neurons of the inferior olivary nucleus depend on *Ptf1a* for fate determination (Yamada et al., 2007). We therefore assessed a possible interaction between Olig3 and Ptf1a in overexpression experiments. The hindbrains of chick embryos were electroporated in ovo at Hamburger-Hamilton stage 16 with an expression construct that produces mouse Olig3, and the embryos were analyzed 48 hours later. On the electroporated side, we observed a pronounced decrease in the numbers of Lbx1$^+$ and dorsal Pax2$^+$ neurons (Fig. 6A,B; quantification in Fig. 6D). This was accompanied by a suppression of Ptf1a (Fig. 6C,D). Electroporation of a Ptf1a expression construct had little effect on the generation of Foxd3$^+$ neurons, and electroporation of an Olig3 expression construct suppressed the generation of Foxd3$^+$ (dA4) neurons (Fig. 6E,F,H). However, co-electroporation of Olig3 and Ptf1a expression constructs induced Foxd3 (Fig. 6G,H). We conclude that Olig3 and Ptf1a can cooperate to induce Foxd3.

An apparent antagonism exists between Olig3 and Lbx1, and Olig3 might exert its function by suppressing Lbx1 (Muller et al., 2005). We therefore investigated whether deficits present in *Olig3* mutants could be rescued in the absence of Lbx1 using *Olig3*; *Lbx1* double-mutant mice (Fig. 6I-O). Foxd3$^+$ dA4 neurons were not formed in *Olig3* mutants, but their generation was rescued in *Olig3*; *Lbx1* double-mutant embryos (Fig. 6I-K). Thus, Olig3 has a permissive role in the determination of the dA4 fate. However, the generation of Phox2b$^+$/Tlx3$^+$ dA3 neurons was not rescued, and at

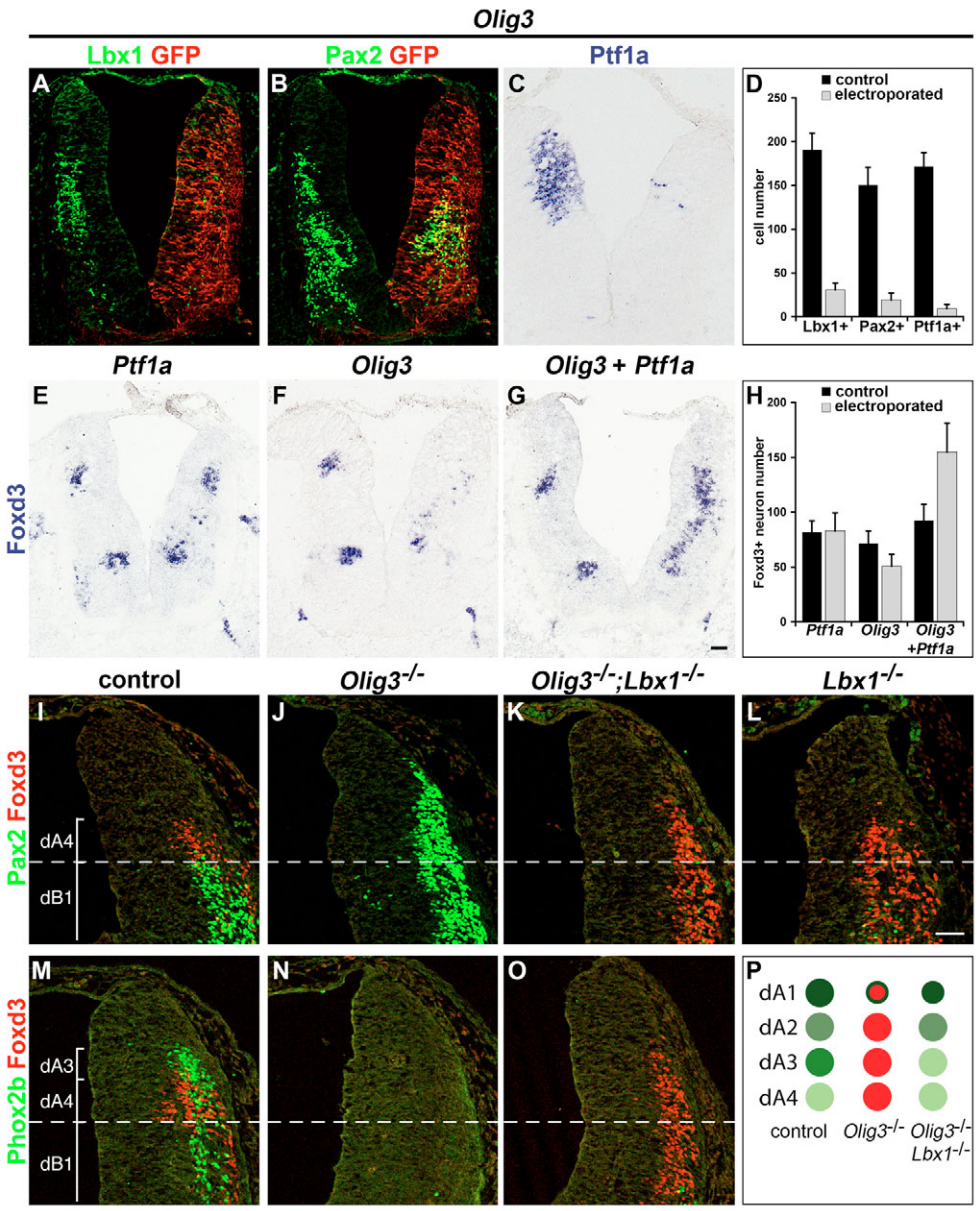

Fig. 6. Cooperation of Olig3 and Ptf1a and permissive functions of Olig3 in the determination of the Foxd3$^+$ dA4 fate. (**A-C**,**E-G**) Chick hindbrains electroporated with mouse Olig3 (A-C,F), Ptf1a (E), Olig3 and Ptf1a (G). Effects were assessed by immunohistochemistry using antibodies against Lbx1 (A) or Pax2 (B), or by in situ hybridization using probes specific for *Ptf1a* (C) or *Foxd3* (E-G). In addition, a GFP vector was co-electroporated to identify electroporated cells. Note that A and B show the same section stained with antibodies against Lbx1, Pax2 and GFP; A and B display the Lbx1/GFP and Pax2/GFP signals, respectively. (**D**,**H**) Quantification of cells that expressed particular transcription factors in the dorsal part of the chick caudal medulla oblongata. (**I-O**) Comparison of the dorsal alar plate in control (I,M), *Olig3* mutant (J,N), *Olig3*; *Lbx1* double-mutant (K,O) and *Lbx1* mutant (L) mice, using antibodies against Foxd3 and Pax2 (I-L) and Foxd3 and Phox2b (M-O). The dashed line indicates the ventral limit of *Oligo3* expression. (**P**) Summary of neuronal types observed in control, *Olig3* and *Olig3*; *Lbx1* mutant mice. The colors indicate the neural subtypes defined in Fig. 1I by their transcription factor code. Scale bars: 50 μm.

their expense ectopic Foxd3$^+$ neurons appeared (Fig. 6M-O and data not shown; summary in Fig. 6P). Lbx1 repression alone cannot therefore explain Olig3 function(s) in the determination of the dA3 fate.

dA3 neurons express Phox2b and Tlx3, and generate the nucleus of the solitary tract and the area postrema (Qian et al., 2001; Dauger et al., 2003). These neurons arose in the dorsal alar plate and migrated ventrally to settle lateral to vagal motoneurons that express Phox2b but not Tlx3 (Fig. 7A,B; the arrows point towards vagal motoneurons and the asterisk indicates the future neurons of the nucleus of the solitary tract) (Dauger et al., 2003). Subsequent morphogenetic movements of the hindbrain resulted in a dorsal location of the Phox2b$^+$/Tlx3$^+$ neurons, close to the midline (Fig. 7C) (Dauger et al., 2003). In rhombomeres 7 and 4-6 of *Olig3* mutant mice, Phox2b$^+$/Tlx3$^+$ neurons were not formed (Fig. 7D and Fig. 3F). At E13.5, we observed no Phox2b$^+$ neurons at the site of the future nucleus of the solitary tract in *Olig3* mutant mice (Fig. 7E). At E18.5, we could not discern Phox2b$^+$/Tlx3$^+$ neurons in the nucleus of the solitary tract (Fig. 7F). In addition, the area postrema was not formed (Fig. 4F). By contrast, vagal motoneurons (Phox2b$^+$ and Tlx3$^-$) were present at the expected location at all developmental stages (Fig. 7, arrows). We conclude that the fate of Phox2b$^+$/Tlx3$^+$ dA3 neurons was not correctly determined in *Olig3* mutant mice; as a consequence, the nucleus of the solitary tract and the area postrema were absent.

Lhx2/9$^+$ (dA1) neurons arise from Math1$^+$ cells close to the roof plate (Fig. 2A,I; Fig. 8A) (Bermingham et al., 2001). In *Olig3* mutant mice, we detected Lhx2/9$^+$ cells that arose at the dorsal lip (Fig. 2B and Fig. 8B). These neurons ectopically expressed Lbx1, and we denote them as dA1* (Fig. 2). Quantification showed that Lhx2/9$^+$ neurons were generated at reduced numbers in *Olig3* mutant as compared with control mice (Fig. 8A-C). In normal development, Lhx2/9$^+$ neurons migrate ventrally in a superficial migratory stream (Fig. 8A). During migration and when they settle, Lhx2/9$^+$ neurons of rhombomere 7 express Barhl1/2 and generate the lateral reticular and external cuneate nuclei (Saito et al., 1998; Bermingham et al., 2001). In situ hybridization demonstrated the presence of Barhl1$^+$ neurons at

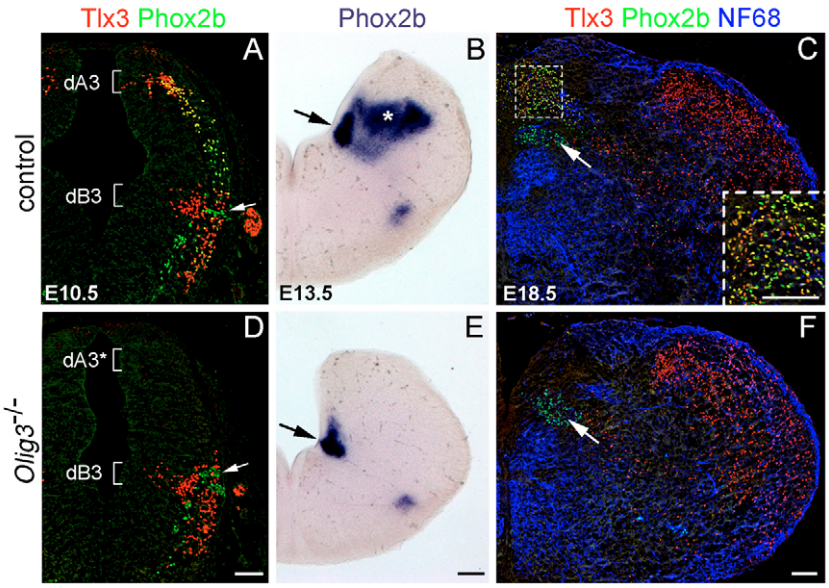

Fig. 7. dA3 neurons and their derivative, the nucleus of the solitary tract, are not generated in *Olig3* mutant mice. The alar plate of rhombomere 7 of control (A-C) and *Olig3* mutant (D-F) mice at E10.5 (A,D), E13.5 (B,E) and E18.5 (C,F). Arrows indicate vagal motoneurons. (**A**,**D**) Immunohistological analysis using antibodies against Phox2b and Tlx3. In control embryos at E10.5, Phox2b$^+$/Tlx3$^+$ marked dA3 neurons (bracket), Phox2b$^+$/Tlx3$^-$ marked vagal motoneurons (arrow), and Phox2b$^-$/Tlx3$^+$ marked dB3 neurons (bracket). In *Olig3* mutant mice, dA3 neurons were absent. (**B**,**E**) In situ hybridization using a *Phox2b*-specific probe. In control embryos at E13.5, dA3 neurons (asterisk) were positioned dorsal to the vagal motoneurons (arrow). dA3 neurons were absent in *Olig3* mutant mice. (**C**,**F**) Immunohistological analysis using antibodies against Tlx3, Phox2b and NF68. In *Olig3* mutant mice, the Phox2b$^+$/Tlx3$^+$ neurons (inset in C) of the nucleus of the solitary tract were absent, but vagal motoneurons (arrows) were present. Scale bars: 100 μm in D,E; 200 μm in F.

the positions of the lateral reticular and external cuneate nuclei in *Olig3* mutant mice, but compared with control mice the size of these nuclei was reduced (Fig. 8D-I). We conclude that Lhx2/9$^+$ dA1* neurons of *Olig3* mutant mice misexpressed Lbx1, but assembled at the sites of the lateral reticular and external cuneate nuclei. These nuclei were reduced in size, reflecting the small numbers of Lhx2/9$^+$ dA1* neurons generated in *Olig3* mutants.

DISCUSSION

The bHLH factor Olig3 is expressed in a dorsal ventricular zone of the hindbrain that gives rise to several neuronal types that we denote as class A neurons. Genetic lineage tracing demonstrated that Olig3$^+$ cells give rise to the nucleus of the solitary tract and to precerebellar nuclei, such as the inferior olivary nuclei. In *Olig3* mutant mice, the fate of class A neurons was not correctly determined (see Fig. 9 for a summary of the fate changes observed in rhombomeres 7 and 4-6). This resulted in the absence, or reduced size, of nuclei that derive from class A neurons. At the expense of class A neurons, ectopic Lbx1$^+$ neurons arose. Conversely, we found that the misexpression of *Olig3* in the chick hindbrain suppressed the appearance of Lbx1$^+$ neurons. Olig3 and Ptf1a are both essential for the specification of climbing fiber neurons of the inferior olivary nucleus [compare Yamada et al. (Yamada et al., 2007) with this study]. Co-electroporation of Olig3 and Ptf1a expression vectors induced Foxd3, a molecular characteristic of climbing fiber neurons of the inferior olivary nucleus (see Fig. 9 for a model of Olig3 function).

Derivatives of Olig3$^+$ progenitor cells

We show here that Olig3 is expressed in the ventricular zone of the dorsal alar plate of the hindbrain. The expression of the bHLH factors Math1, Ngn1, Mash1 and Ptf1a further subdivided the Olig3$^+$ progenitor domain. We used genetic lineage tracing to follow the fate of the Olig3$^+$ cells, which contributed to the nucleus of the solitary tract and to precerebellar nuclei including the lateral reticular, external cuneate and inferior olivary nuclei.

Climbing fiber neurons of the inferior olivary nucleus arise in the dorsal alar plate, and undergo extensive migration before they settle in the ventral medulla oblongata (Cobos et al., 2001; Bloch-Gallego et al., 2005). These neurons derive from Ptf1a$^+$ progenitors and depend on Ptf1a for determination of their fate (Yamada et al., 2007). We show here that Olig3 is also essential to determine the fate of these neurons. The nucleus of the solitary tract and the area postrema are generated by dA3 viscerosensory relay neurons that co-express Phox2b and Tlx3 (Qian et al., 2001; Dauger et al., 2003) (this study), which appear to arise from a ventricular zone containing Olig3$^+$ and Mash1$^+$ cells in rhombomeres 4-7. In *Olig3* mutant mice, the fate of dA3 viscerosensory relay neurons was not correctly determined, and

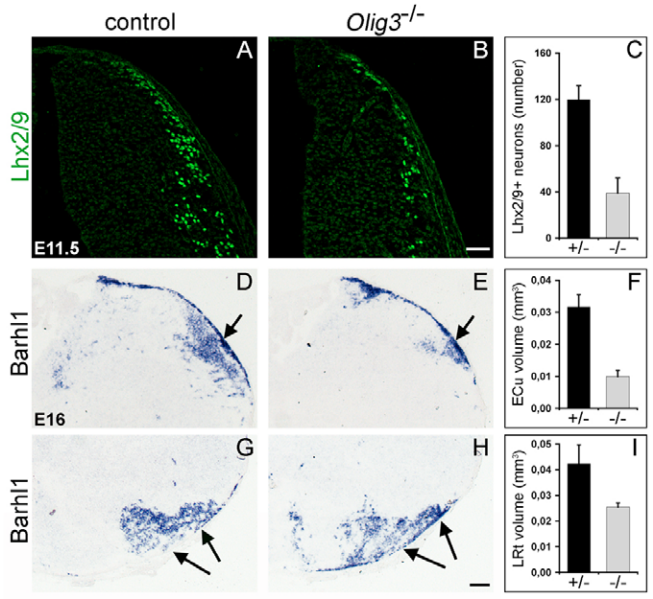

Fig. 8. Development of dA1 neurons in *Olig3* mutant mice. Analyses of rhombomere 7 of control (A,D,G) and *Olig3* mutant (B,E,H) mice. (**A**,**B**) Immunohistological analysis using anti-Lhx2/9 antibodies at E11.5. (**C**) Quantification of Lhx2/9$^+$ neuron numbers. (**D**,**E**,**G**,**H**) In situ hybridization analysis using a probe specific for *Barhl1*. Arrows indicate external cuneate nuclei in D,E, and the lateral reticular nuclei in G,H. (**F**,**I**) Morphometric analysis of the volume of external cuneate (F) and lateral reticular nuclei (I) of control (+/–) and *Olig3* mutant mice (–/–). Scale bars: 50 μm in B; 100 μm in H.

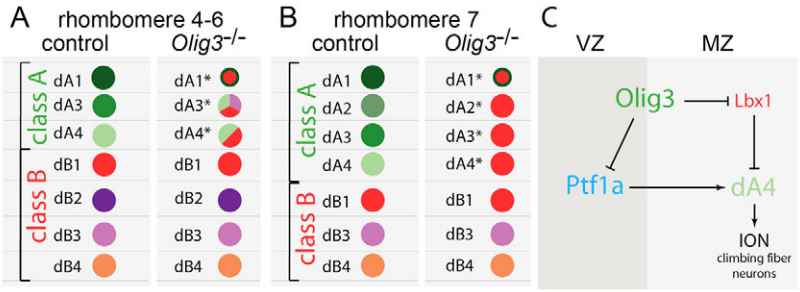

Fig. 9. Summary of the changes in neuronal fate in *Olig3* mutant mice. Summary of the neuronal types generated in the alar plate of control and *Olig3* mutant mice in (**A**) rhombomeres 4-6 and (**B**) rhombomere 7. In *Olig3* mutant mice, the fate of class A neurons was not correctly determined, and ectopic Lbx1$^+$ neurons appear instead. (**C**) Model of Olig3 function in fate determination of dA4 climbing fiber neurons. Olig3 and Ptf1a cooperate to induce the dA4 fate; Olig3 exerts its function primarily by suppressing Lbx1. Ptf1a is known to suppress Tlx3 (Glasgow et al., 2005; Mizuguchi et al., 2006; Hori et al., 2008), and the dA4 fate might require the suppression of Lbx1 and Tlx3 by Olig3 and Ptf1a, respectively. Olig3 also appears to suppress Ptf1a; it should be noted that in normal development, Olig3 and Ptf1a are only transiently co-expressed in cells that locate to the border of the ventricular zone (VZ) and mantle zone (MZ). The colors indicate the neuronal subtypes defined in Fig. 1I by their transcription factor code.

the nucleus of the solitary tract and the area postrema were not formed. Mossy fiber neurons of the lateral reticular, external cuneate, pontine, reticulotegmental nuclei, and the neurons of the parabrachial nucleus appear to derive from cells expressing Math1 and Olig3 at the rhombic lip (Bermingham et al., 2001; Li et al., 2004; Wang et al., 2005; Farago et al., 2006) (this study). Lhx2/9 neurons arose in *Olig3* mutant mice at reduced numbers, and lateral reticular, external cuneate, pontine, reticulotegmental and parabrachial nuclei were small. Thus, Lhx2/9$^+$ neurons of *Olig3* mutant mice appeared to retain the ability to migrate and differentiate, despite the fact that they ectopically expressed Lbx1.

In summary, the functional characterization of genes and genetic lineage tracing revealed derivatives of several class A neuronal subtypes: dA1, mossy fiber neurons of lateral reticular and external cuneate nucleus in rhombomere 7 and additional derivatives in more-anterior rhombomeres (Wang et al., 2005); dA3, viscerosensory relay neurons of the nucleus of the solitary tract and the area postrema (Qian et al., 2001; Dauger et al., 2003); and dA4, climbing fiber neurons of the inferior olivary nucleus in rhombomere 7 (Yamada et al., 2007). dA2 neurons appear to arise from a ventricular zone that expresses Olig3 and Ngn1, which exists in rhombomere 7 but not in other hindbrain segments (Landsberg et al., 2005). With the available markers, we have not as yet been able to trace dA2 neurons during development. The cuneate nucleus is generated by an as yet unidentified neuronal type that derives from Olig3$^+$ progenitors. Future experiments, for instance genetic lineage tracing of Ngn1$^+$ cells, might help to assign the fate of dA2 neurons.

Olig3, Ptf1a and neuronal fate determination

In the dorsal spinal cord and hindbrain, Ptf1a is expressed in a ventricular zone that gives rise to Lbx1$^+$/Pax2$^+$ inhibitory and dA4 climbing fiber excitatory neurons of the inferior olivary nucleus, and Ptf1a is essential to determine the fate of both neuronal types (Glasgow et al., 2005; Hoshino et al., 2005; Yamada et al., 2007). Electroporation of Ptf1a leads to the appearance of supernumerary inhibitory neurons (Hoshino et al., 2005; Wildner et al., 2006; Hori et al., 2008). To determine an inhibitory neuronal fate, Ptf1a forms a trimeric complex consisting of Ptf1a, Rbpj and an E-box factor, such as Tcf12 (Hori et al., 2008). Rbpj is best known as the major transcriptional mediator of Notch signaling, but its role in the determination of an inhibitory neuronal fate appears to be independent of Notch (Hori et al., 2008). It is currently unclear whether a Ptf1a-Rbpj-Tcf12 complex also functions in the fate determination of climbing fiber neurons.

In *Olig3* mutant mice, the Ptf1a expression domain was expanded, and supernumerary inhibitory neurons appeared. In control mice, the dorsal Olig3$^+$ domain was substantial in size early on (E11.5), but was markedly smaller at later developmental stages. Accordingly, the domain that generated misspecified neurons in *Olig3* mutant mice became smaller as development proceeded. We found that even at E18.5, the number of Pax2$^+$/Lbx1$^+$ or Gad1$^+$ neurons was increased in the caudal medulla oblongata of the mutant mice. The physiological consequence of the increased number of inhibitory neurons is unclear. Homozygous *Olig3* mutant mice become cyanotic and die shortly after birth, apparently because they are unable to breathe. Breathing is controlled by a network of neurons in the brainstem (Feldman et al., 2003; Dubreuil et al., 2008), and it is tempting to speculate that an increased inhibition is responsible for the breathing deficit of *Olig3* mutant mice.

Olig3 and Ptf1a are essential to determine the fate of dA4 climbing fiber neurons of the inferior olivary nucleus, which appear to arise from a ventricular domain that contains cells expressing Ptf1a and Olig3 in rhombomere 7. We therefore tested whether the two factors cooperate, and co-electroporated Ptf1a and Olig3 expression vectors in the chick hindbrain. This led to an induction of Foxd3, a molecular characteristic of climbing fiber neurons. We therefore propose that Ptf1a and Olig3 cooperate to determine the fate of the climbing fiber neurons. In such experiments, ectopic Foxd3$^+$ neurons were not observed close to the floor and roof plate, indicating that the two factors act in a context-dependent manner. Our model, a cooperation of Ptf1a and Olig3 during fate determination of climbing fiber neurons, is in apparent contradiction with the observed suppression of Ptf1a by Olig3. However, it should be noted that, in normal development, we found Olig3 to be expressed in Ki67$^-$ cells located laterally in the ventricular domain that appears to generate Foxd3$^+$ climbing fiber neurons, indicating that Olig3 is transiently expressed in progenitors that have left the cell cycle and begun to differentiate. Ptf1a is expressed more broadly in this domain, and only a few cells co-expressed Ptf1a and Olig3 (Fig. 1E). Onset of Ptf1a and Olig3 expression thus appear to occur in distinct phases of the cell cycle, and result in a transient co-expression of the two factors in normal development. Distinct time courses of Ptf1a and Olig3 expression could thus explain the data.

Viscerosensory dA3 neurons and climbing fiber dA4 neurons were not specified in *Olig3* mutant mice, and Lbx1$^+$ neurons arose at their expense. We tested whether Olig3 exerts its role solely by suppressing Lbx1. If this were the case, the changed fate determination of dA3 and dA4 neurons in *Olig3* mutant mice should be reverted by the *Lbx1* mutation. Analysis of *Olig3*; *Lbx1* double-mutant mice demonstrated that this was indeed the case for dA4, but not dA3, neurons. Thus, Olig3 and Ptf1a together induce a dA4 fate, but the primary role of Olig3 in this process is the suppression of Lbx1. Ptf1a is known to suppress Tlx3 (Glasgow et al., 2005; Mizuguchi et al., 2006; Hori et al., 2008), and Phox2b$^+$ viscerosensory neurons are not generated in *Tlx3* mutant mice (Qian et al., 2001). It is tempting to speculate that the determination of the Foxd3$^+$ dA4 fate depends on the suppression of Lbx1 and Tlx3 by Olig3 and Ptf1a, respectively.

Olig3 and the molecular mechanisms of neuronal fate determination in the spinal cord and hindbrain

Despite the greater complexity of neuronal types in the hindbrain as compared with the spinal cord, and the distinct functions of hindbrain and spinal neurons, neurons with similar molecular characteristics are frequently generated in longitudinal columns that span the spinal cord and reach into the hindbrain. This indicates that similarities exist in the mechanisms that determine neuronal fates in the two units. Olig3 is expressed in the spinal cord and hindbrain, and our analyses show some similarities in Olig3 function in these two units. In particular, Olig3 marks the dorsal ventricular zone in both, and a dorsal expansion of Lbx1 expression was observed in the spinal cord and hindbrain of *Olig3* mutant mice. Furthermore, in the spinal cord and hindbrain of the chick, ectopic expression of Olig3 suppresses the emergence of Lbx1$^+$ neurons. Thus, several aspects of Olig3 function are conserved in the spinal cord and hindbrain [compare Fig. 9 with Muller et al.] (Muller et al., 2005).

We thank Michael Strehle for help with manuscript preparation; Elvira Rhode for help with ES cell culture; Petra Stallerow and Claudia Päseler for help with animal husbandry; Boris Jerchow and Katja Becker for blastocyst injections; and Jean-Francois Brunet, Christo Goridis, David Anderson, Martyn Goulding, Jane Johnson, Eric Turner and Tom Jessell for gifts of antibodies and probes. We gratefully acknowledge Jane Johnson and Jean-Francois Brunet for discussions and sharing of unpublished data. C.B. and T.M. are supported by a grant from the DFG (SFB 665).

Supplementary material

Supplementary material for this article is available at
http://dev.biologists.org/cgi/content/full/136/2/295/DC1

References

Altman, J. and Bayer, S. A. (1980). Development of the brain stem in the rat. I. Thymidine-radiographic study of the time of origin of neurons of the lower medulla. *J. Comp. Neurol.* **194**, 1-35.

Altman, J. and Bayer, S. A. (1987). Development of the precerebellar nuclei in the rat: I. The precerebellar neuroepithelium of the rhombencephalon. *J. Comp. Neurol.* **257**, 477-489.

Arnett, H. A., Fancy, S. P., Alberta, J. A., Zhao, C., Plant, S. R., Kaing, S., Raine, C. S., Rowitch, D. H., Franklin, R. J. and Stiles, C. D. (2004). bHLH transcription factor Olig1 is required to repair demyelinated lesions in the CNS. *Science* **306**, 2111-2115.

Bermingham, N. A., Hassan, B. A., Wang, V. Y., Fernandez, M., Banfi, S., Bellen, H. J., Fritzsch, B. and Zoghbi, H. Y. (2001). Proprioceptor pathway development is dependent on Math1. *Neuron* **30**, 411-422.

Bertrand, N., Castro, D. S. and Guillemot, F. (2002). Proneural genes and the specification of neural cell types. *Nat. Rev. Neurosci.* **3**, 517-530.

Blessing, W. W. (1997). *The Lower Brainstem and Bodily Homeostasis*: New York: Oxford University Press.

Bloch-Gallego, E., Causeret, F., Ezan, F., Backer, S. and Hidalgo-Sanchez, M. (2005). Development of precerebellar nuclei: instructive factors and intracellular mediators in neuronal migration, survival and axon pathfinding. *Brain Res. Brain Res. Rev.* **49**, 253-266.

Branda, C. S. and Dymecki, S. M. (2004). Talking about a revolution: the impact of site-specific recombinases on genetic analyses in mice. *Dev. Cell* **6**, 7-28.

Brohmann, H., Jagla, K. and Birchmeier, C. (2000). The role of Lbx1 in migration of muscle precursor cells. *Development* **127**, 437-445.

Brunet, J. F. and Ghysen, A. (1999). Deconstructing cell determination: proneural genes and neuronal identity. *BioEssays* **21**, 313-318.

Byun, J., Verardo, M. R., Sumengen, B., Lewis, G. P., Manjunath, B. S. and Fisher, S. K. (2006). Automated tool for the detection of cell nuclei in digital microscopic images: application to retinal images. *Mol. Vis.* **12**, 949-960.

Cambronero, F. and Puelles, L. (2000). Rostrocaudal nuclear relationships in the avian medulla oblongata: a fate map with quail chick chimeras. *J. Comp. Neurol.* **427**, 522-545.

Cheng, L., Samad, O. A., Xu, Y., Mizuguchi, R., Luo, P., Shirasawa, S., Goulding, M. and Ma, Q. (2005). Lbx1 and Tlx3 are opposing switches in determining GABAergic versus glutamatergic transmitter phenotypes. *Nat. Neurosci.* **8**, 1510-1515.

Cobos, I., Shimamura, K., Rubenstein, J. L., Martinez, S. and Puelles, L. (2001). Fate map of the avian anterior forebrain at the four-somite stage, based on the analysis of quail-chick chimeras. *Dev. Biol.* **239**, 46-67.

Dauger, S., Pattyn, A., Lofaso, F., Gaultier, C., Goridis, C., Gallego, J. and Brunet, J. F. (2003). Phox2b controls the development of peripheral chemoreceptors and afferent visceral pathways. *Development* **130**, 6635-6642.

Ding, L., Takebayashi, H., Watanabe, K., Ohtsuki, T., Tanaka, K. F., Nabeshima, Y., Chisaka, O., Ikenaka, K. and Ono, K. (2005). Short-term lineage analysis of dorsally derived Olig3 cells in the developing spinal cord. *Dev. Dyn.* **234**, 622-632.

Dubreuil, V., Hirsch, M. R., Jouve, C., Brunet, J. F. and Goridis, C. (2002). The role of Phox2b in synchronizing pan-neuronal and type-specific aspects of neurogenesis. *Development* **129**, 5241-5253.

Dubreuil, V., Ramanantsoa, N., Trochet, D., Vaubourg, V., Amiel, J., Gallego, J., Brunet, J. F. and Goridis, C. (2008). A human mutation in Phox2b causes lack of CO2 chemosensitivity, fatal central apnea, and specific loss of parafacial neurons. *Proc. Natl. Acad. Sci. USA* **105**, 1067-1072.

Farago, A. F., Awatramani, R. B. and Dymecki, S. M. (2006). Assembly of the brainstem cochlear nuclear complex is revealed by intersectional and subtractive genetic fate maps. *Neuron* **50**, 205-218.

Farley, F. W., Soriano, P., Steffen, L. S. and Dymecki, S. M. (2000). Widespread recombinase expression using FLPeR (flipper) mice. *Genesis* **28**, 106-110.

Feil, R., Wagner, J., Metzger, D. and Chambon, P. (1997). Regulation of Cre recombinase activity by mutated estrogen receptor ligand-binding domains. *Biochem. Biophys. Res. Commun.* **237**, 752-757.

Feldman, J. L., Mitchell, G. S. and Nattie, E. E. (2003). Breathing: rhythmicity, plasticity, chemosensitivity. *Annu. Rev. Neurosci.* **26**, 239-266.

Fienberg, A. A., Utset, M. F., Bogarad, L. D., Hart, C. P., Awgulewitsch, A., Ferguson-Smith, A., Fainsod, A., Rabin, M. and Ruddle, F. H. (1987). Homeo box genes in murine development. *Curr. Top. Dev. Biol.* **23**, 233-256.

Filippi, A., Tiso, N., Deflorian, G., Zecchin, E., Bortolussi, M. and Argenton, F. (2005). The basic helix-loop-helix olig3 establishes the neural plate boundary of the trunk and is necessary for development of the dorsal spinal cord. *Proc. Natl. Acad. Sci. USA* **102**, 4377-4382.

Fraser, S., Keynes, R. and Lumsden, A. (1990). Segmentation in the chick embryo hindbrain is defined by cell lineage restrictions. *Nature* **344**, 431-435.

Glasgow, S. M., Henke, R. M., Macdonald, R. J., Wright, C. V. and Johnson, J. E. (2005). Ptf1a determines GABAergic over glutamatergic neuronal cell fate in the spinal cord dorsal horn. *Development* **132**, 5461-5469.

Hori, K., Cholewa-Waclaw, J., Nakada, Y., Glasgow, S. M., Masui, T., Henke, R. M., Wildner, H., Martarelli, B., Beres, T. M., Epstein, J. A. et al. (2008). A nonclassical bHLH Rbpj transcription factor complex is required for specification of GABAergic neurons independent of Notch signaling. *Genes Dev.* **22**, 166-178.

Hoshino, M., Nakamura, S., Mori, K., Kawauchi, T., Terao, M., Nishimura, Y. V., Fukuda, A., Fuse, T., Matsuo, N., Sone, M. et al. (2005). Ptf1a, a bHLH transcriptional gene, defines GABAergic neuronal fates in cerebellum. *Neuron* **47**, 201-213.

Joyner, A. L. and Zervas, M. (2006). Genetic inducible fate mapping in mouse: establishing genetic lineages and defining genetic neuroanatomy in the nervous system. *Dev. Dyn.* **235**, 2376-2385.

Krumlauf, R., Marshall, H., Studer, M., Nonchev, S., Sham, M. H. and Lumsden, A. (1993). Hox homeobox genes and regionalisation of the nervous system. *J. Neurobiol.* **24**, 1328-1340.

Landsberg, R. L., Awatramani, R. B., Hunter, N. L., Farago, A. F., DiPietrantonio, H. J., Rodriguez, C. I. and Dymecki, S. M. (2005). Hindbrain rhombic lip is comprised of discrete progenitor cell populations allocated by Pax6. *Neuron* **48**, 933-947.

Li, S., Qiu, F., Xu, A., Price, S. M. and Xiang, M. (2004). Barhl1 regulates migration and survival of cerebellar granule cells by controlling expression of the neurotrophin-3 gene. *J. Neurosci.* **24**, 3104-3114.

Lu, Q. R., Sun, T., Zhu, Z., Ma, N., Garcia, M., Stiles, C. D. and Rowitch, D. H. (2002). Common developmental requirement for Olig function indicates a motor neuron/oligodendrocyte connection. *Cell* **109**, 75-86.
Machold, R. and Fishell, G. (2005). Math1 is expressed in temporally discrete pools of cerebellar rhombic-lip neural progenitors. *Neuron* **48**, 17-24.
Marin, F. and Puelles, L. (1995). Morphological fate of rhombomeres in quail/chick chimeras: a segmental analysis of hindbrain nuclei. *Eur. J. Neurosci.* **7**, 1714-1738.
Mizuguchi, R., Sugimori, M., Takebayashi, H., Kosako, H., Nagao, M., Yoshida, S., Nabeshima, Y., Shimamura, K. and Nakafuku, M. (2001). Combinatorial roles of olig2 and neurogenin2 in the coordinated induction of pan-neuronal and subtype-specific properties of motoneurons. *Neuron* **31**, 757-771.
Mizuguchi, R., Kriks, S., Cordes, R., Gossler, A., Ma, Q. and Goulding, M. (2006). Ascl1 and Gsh1/2 control inhibitory and excitatory cell fate in spinal sensory interneurons. *Nat. Neurosci.* **9**, 770-778.
Muller, T., Brohmann, H., Pierani, A., Heppenstall, P. A., Lewin, G. R., Jessell, T. M. and Birchmeier, C. (2002). The homeodomain factor lbx1 distinguishes two major programs of neuronal differentiation in the dorsal spinal cord. *Neuron* **34**, 551-562.
Muller, T., Anlag, K., Wildner, H., Britsch, S., Treier, M. and Birchmeier, C. (2005). The bHLH factor Olig3 coordinates the specification of dorsal neurons in the spinal cord. *Genes Dev.* **19**, 733-743.
Novitch, B. G., Chen, A. I. and Jessell, T. M. (2001). Coordinate regulation of motor neuron subtype identity and pan-neuronal properties by the bHLH repressor Olig2. *Neuron* **31**, 773-789.
Pattyn, A., Goridis, C. and Brunet, J. F. (2000). Specification of the central noradrenergic phenotype by the homeobox gene Phox2b. *Mol. Cell. Neurosci.* **15**, 235-243.
Pattyn, A., Guillemot, F. and Brunet, J. F. (2006). Delays in neuronal differentiation in Mash1/Ascl1 mutants. *Dev. Biol.* **295**, 67-75.
Qian, Y., Fritzsch, B., Shirasawa, S., Chen, C. L., Choi, Y. and Ma, Q. (2001). Formation of brainstem (nor)adrenergic centers and first-order relay visceral sensory neurons is dependent on homeodomain protein Rnx/Tlx3. *Genes Dev.* **15**, 2533-2545.
Ross, S. E., Greenberg, M. E. and Stiles, C. D. (2003). Basic helix-loop-helix factors in cortical development. *Neuron* **39**, 13-25.
Saito, T., Sawamoto, K., Okano, H., Anderson, D. J. and Mikoshiba, K. (1998). Mammalian BarH homologue is a potential regulator of neural bHLH genes. *Dev. Biol.* **199**, 216-225.
Sieber, M. A., Storm, R., Martinez-de-la-Torre, M., Muller, T., Wende, H., Reuter, K., Vasyutina, E. and Birchmeier, C. (2007). Lbx1 acts as a selector gene in the fate determination of somatosensory and viscerosensory relay neurons in the hindbrain. *J. Neurosci.* **27**, 4902-4909.
Soriano, P. (1999). Generalized lacZ expression with the ROSA26 Cre reporter strain. *Nat. Genet.* **21**, 70-71.
Takebayashi, H., Nabeshima, Y., Yoshida, S., Chisaka, O. and Ikenaka, K. (2002a). The basic helix-loop-helix factor olig2 is essential for the development of motoneuron and oligodendrocyte lineages. *Curr. Biol.* **12**, 1157-1163.
Takebayashi, H., Ohtsuki, T., Uchida, T., Kawamoto, S., Okubo, K., Ikenaka, K., Takeichi, M., Chisaka, O. and Nabeshima, Y. (2002b). Non-overlapping expression of Olig3 and Olig2 in the embryonic neural tube. *Mech. Dev.* **113**, 169-174.
Wang, V. Y., Rose, M. F. and Zoghbi, H. Y. (2005). Math1 expression redefines the rhombic lip derivatives and reveals novel lineages within the brainstem and cerebellum. *Neuron* **48**, 31-43.
Wildner, H., Muller, T., Cho, S. H., Brohl, D., Cepko, C. L., Guillemot, F. and Birchmeier, C. (2006). dILA neurons in the dorsal spinal cord are the product of terminal and non-terminal asymmetric progenitor cell divisions, and require Mash1 for their development. *Development* **133**, 2105-2113.
Wilkinson, D. G., Bhatt, S., Cook, M., Boncinelli, E. and Krumlauf, R. (1989). Segmental expression of Hox-2 homoeobox-containing genes in the developing mouse hindbrain. *Nature* **341**, 405-409.
Yamada, M., Terao, M., Terashima, T., Fujiyama, T., Kawaguchi, Y., Nabeshima, Y. and Hoshino, M. (2007). Origin of climbing fiber neurons and their developmental dependence on Ptf1a. *J. Neurosci.* **27**, 10924-10934.
Zechner, D., Muller, T., Wende, H., Walther, I., Taketo, M. M., Crenshaw, E. B., 3rd, Treier, M., Birchmeier, W. and Birchmeier, C. (2007). Bmp and Wnt/beta-catenin signals control expression of the transcription factor Olig3 and the specification of spinal cord neurons. *Dev. Biol.* **303**, 181-190.
Zhou, Q. and Anderson, D. J. (2002). The bHLH transcription factors OLIG2 and OLIG1 couple neuronal and glial subtype specification. *Cell* **109**, 61-73.
Zhou, Q., Choi, G. and Anderson, D. J. (2001). The bHLH transcription factor Olig2 promotes oligodendrocyte differentiation in collaboration with Nkx2.2. *Neuron* **31**, 791-807.